AKADÉMIAI KIADÓ

UNIVERSITY of DEBRECEN

International Review of Applied Sciences and Engineering

15 (2024) 2, 211–220

DOI:
10.1556/1848.2023.00706

REVIEW PAPER

Adaptive synergetic control for electronic throttle valve system

Ahmed F. Mutlak* and Amjad Jaleel Humaidi

Control and Systems Engineering Department, University of Technology, Baghdad, Iraq

Received: July 15, 2023 • Accepted: September 24, 2023
Published online: November 21, 2023

ABSTRACT

This study has developed adaptive synergetic control (ASC) algorithm to control the angular position of moving plate in the electronic throttle valve (ETV) system. This control approach is inspired by synergetic control theory. The adaptive controller has addressed the problem of variation in systems parameters. The control design includes two elements: the control law and adaptive law. The adaptive law is developed based on Lyupunov stability analysis of the controlled system, and it is responsible for estimating the potential uncertainties in the system. The effectiveness of the proposed adaptive synergetic control has been verified by numerical simulation using MATLAB/Simulink. The results showed that the ASC algorithm could give good tracking performance in the presence of uncertainty perturbations. In addition, a comparison study has been made to compare the tracking performance of ASC and that based on conventional synergetic control (CSC) for the ETV system. The simulated results showed that the performance of ASC outperforms that based on CSC. Moreover, the results showed that the estimation errors between the actual and estimated uncertainties are bounded and there is no drift in the developed adaptive law of ASC.

KEYWORDS

electronic throttle valve, synergetic control, adaptive control, uncertainty, stability analysis

1. INTRODUCTION

The electronic throttle valve device is a modern technology in recent industrial and automotive applications. It serves to manage the air flow in gasoline-powered engines to achieve optimal air-fuel mixtures, to minimize emissions and to maximize fuel economy [1]. Due to complex nonlinearities, it is difficult to find exact and reliable physical models. Therefore, the control of throttle valve system is a challenging problem and a robust controller is required to cope with built-in uncertainties. The valve of ETV must be regulated rapidly without overshoot to ensure bounded position errors. The electronic throttle valve consists of servo motor, motor pinion gear, valve plates, dynamic spring, and position sensor (see Fig. 1).

Synergetic controls take advantage of the potential of open systems to self-organize. The theory implies a holistic philosophy of regulated dynamic interactions between energy, matter, and information, which is executed by means of both positive and negative feedback. The philosophy of synergetic control design is founded on the notion of dynamic expansion and contraction of the controlled system's state space. The extension of the state space enriches the system dynamics by supplying more information that is essential for enhancing the efficiency of the closed-loop system. In contrast to expansion, constriction of the state space accomplished by the control action eliminates undesirable system dynamics or reduces excessive degrees of freedom. At the stage of control design, these undesirable dynamics are eliminated by inserting dynamic constraints represented as invariant manifolds in the system's state space. In what follows, a brief review of previous works that are most recent and relevant will be presented. Yuan et al. [2] proposed a support vector machine (SVM)-based approximate model control for the electronic throttle. Based on an

*Corresponding author.
E-mail: cse.20.14@uotechnology.edu.iq

AKJournals

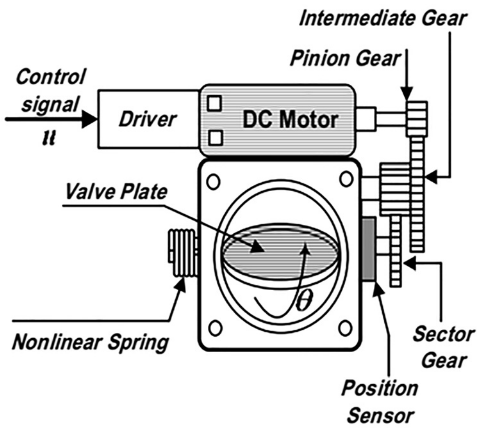

Fig. 1. Schematic of the electronic throttle valve control system

input-output approximation method, the Taylor expansion is used to develop the nonlinear control law such as to avoid complexity in control design, reduction in computation effort, and to perform online adjustment and learning. With a new input–output approximation introduced for the general NARMA model, the approximate control law is defined straightly, and its design by using the SVM is direct without additional training. Honek et al. [3] address a problem with electronic throttle control. The suggested approach method is a discrete PI controller with a feedforward controller and parameters scheduling working together. Dulau and Oltean [4] describe the mathematical modeling of the throttle valve of internal combustion engines. The model is used to create reliable controllers using H2 and H(inf) synthesis All of the simulation scenarios focus attention on the closed-loop system's rightness stability characteristics, even when the plant model is influenced by disturbances. Horn et al. [5] presented controllers for electronic throttle valves, using concepts of sliding-mode control to be applied. Standard integrating sliding-mode controllers are in opposition to super-twisting algorithms, which are higher order concepts. Zeng & Wan [6] designed a nonlinear PID controller for the position control of the throttle valve. With the changing system error, it continuously modifies the controller's proportional gain P, integral gain I, and differential gain D. Son Tran & Ngoc Anh Dang [7] suggested a control strategy using a Model Reference Adaptive System-based Learning Feed-Forward Controller technique to combine a PD controller with a traditional PID controller to replace it. Combining these techniques will allow the PD controller to manage the valve plate's position while tracking the reference signal by overcoming the nonlinearities in the system. Mercorelli [8] demonstrated how an approximated proportional derivative (PD) regulator may be self-tuned in real time to compensate for tracking error induced by inexact feedback linearization. It is worth noting that the structure of the estimated PD regulator is identical to that of the velocity estimator. The suggested loop control achieves robustness. Thanok et al. [9] developed adaptive cruise control and created an AIT intelligent car. Drive-by-wire technology replaces the mechanical throttle valve control. The position of the throttle valve is controlled by a dc servo motor in the drive-by-wire system. The throttle valve is controlled by a proportional and derivative control algorithm. Loh et al. [10] used the input-output feedback linearization technique to create nonlinear control action for Electronic Throttle Valve system, they compared simulation and real-time implementation output and achieved good outcomes for this specific ETC system. Shibly Ahmed Al-Samarraie et al. [11] developed controller (slide mode) including an estimated perturbation term with a negative sign (to negate it) and a stabilizing term to stabilize the nominal system model. The perturbation term includes unknown external input and nonlinear throttle valve model uncertainty. Humaidi & Hameed [12] developed two adaptive control algorithms for the sliding mode and adaptive backstepping based control of the angular position of the electronic throttle valve plate. Comparison of the two approaches. the establishment of the adaptive law by the utilization of a smoothly switching feature. The Lyapunov theory is utilized to analyze the stability of closed-loop system based on adaptive controller. The control law and adaptive laws of adaptive controller are developed based on Lyapunov stability analysis to guarantee asymptotic stability of adaptive controlled-system.

In the work, design of classic and adaptive synergetic control schemes have been developed to control the position of throttle plate. The following points address the contributions of this study:

1. Design of classic and adaptive control schemes based on synergetic control theory to control the plate angular position of ETV system.
2. Conducting a comparison study in performance between adaptive synergetic control and classic synergetic control.
3. Designing the adaptive law of ASC which ensures boundness of estimated states or to avoid the drift of adaptive gains.

The rest of the article is organized in five sections. The second section presents the state representation of ETV system. The control design for both adaptive and classical synergetic schemes are developed in the third section. The fourth section conducts numerical simulation to validate and assess the performance of both controllers. In the fifth part, the discussion has been conducted. The conclusion and future work has been highlighted in the sixth section.

2. THE DYNAMIC MODEL FOR ELECTRONIC THROTTLE VALVE

Figure 2 shows the details of ETV system. The DC motor is represented by electric circuits. The shaft of DC is linked by gear box, which is used to actuate the plate of the ETV system.

The Kirchhoff's law is used to setup the following equation [10]:

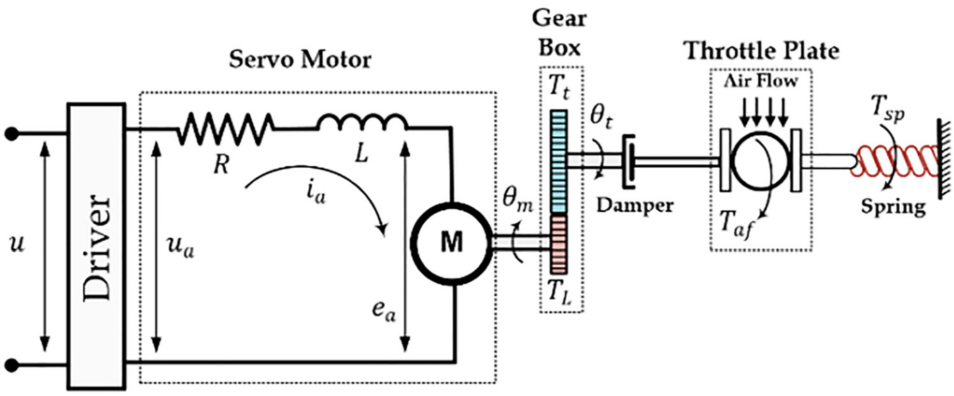

Fig. 2. Circuit diagram of ETV system

$$V_a = K_d u = Ri_a + L\frac{di}{dt} + e_a \quad (1)$$

where V_a is the voltage that is being applied, i_a is the current that is being passed through the motor winding, R represents the armature's resistance, L is the inductance of the armature, K_d is the drive gain, and e_a is the voltage that is being produced by the back electromotive force (e.m.f), which is represented by

$$e_a = K_b\frac{d\theta_m}{dt} \quad (2)$$

where θ_m is the motor's shaft angular position and K_b is the back electromotive force (e.m.f) constant. Since the ratio of L/R is very small, the term associated with coil inductance can be discarded [9]. Consequently, Eq. (3) can be rewritten as [10, 11]:

$$i_a = \frac{K_d}{R}u - \frac{K_b}{R}.\frac{d\theta_m}{dt} \quad (3)$$

The torque developed by the DC motor is expressed as [11]:

$$T_m = K_t.i_a \quad (4)$$

where K_t is the constant motor torque. The developed torque can be expressed in terms of shaft motion as [11, 12]:

$$T_m = J_m\frac{d\theta_m{}^2}{dt^2} + B_m\frac{d\theta_m}{dt} + B_{mo} + T_L \quad (5)$$

where B_m and B_{mo} are the motor shaft's viscosity damping and coefficient of static friction, respectively, J_m represents the inertia of the motor shaft. Via the gear transfer, the transmitted torque T_t tries to counteract the throttle plate movement, spring torque, viscous damping, and static friction of the throttle valve [12]:

$$T_m = J_t\frac{d\theta_t{}^2}{dt^2} + B_t\frac{d\theta_t}{dt} + B_{to} + T_{sp} + T_{af} \quad (6)$$

where B_t and B_{to} are the viscosity damping and static friction coefficients of the throttle valve, T_{af} is the airflow torque, J_t is the throttle inertia, and T_{sp} is the return spring torque described by [13]:

$$T_{sp} = K_{sp}\ (\theta_m + \theta_t) \quad (7)$$

where K_{sp} is the spring's elastic coefficient and θ_t is the throttle angle of the throttle valve.

Equations (3)–(7) can be combined using the gear ratio ($N = \theta_m/\theta_t = T_t/T_L$) to yield:

$$\frac{d\theta_t^2}{dt^2} = -a_1\theta_t - a_1\frac{d\theta_t}{dt} - b_1\ u - f_1 - f_2 - f_3 \quad (8)$$

where θ_t is angle position and $\dot{\theta}_t$ is angular velocity. The airflow torque T_{af} has no effects on the throttle valve's performance and it can be neglected.

Let $x_1 = \theta_t$, $x_2 = \dot{\theta}_t$ and $y = x_1$, the state space variables are given by:

$$\dot{x}_1 = x_2 \quad (9)$$

$$\dot{x}_2 = -a_1x_1 - a_2x_2 + \frac{1}{b1}u + w \quad (10)$$

The above equations are expressed

$$\dot{x} = f + bu \quad (11)$$

where,

$$a_1 = K_{sp}/\left(J_mN^2 + J_t\right) \quad (12)$$

$$a_2 = \left[\left(N^2K_bK_t + R/\left(B_mN^2 + B_t\right)\right)/\left(R/\left(J_mN^2 + J_t\right)\right)\right] \quad (13)$$

$$b_1 = (NK_tK_d)/\left(R/\left(J_mN^2 + J_t\right)\right) \quad (14)$$

$$w = -f_1 - f_2 - f_3 \quad (15)$$

$$f_1 = K_{sp}\theta_0/\left(J_mN^2 + J_t\right) \quad (16)$$

$$f_2 = T_{af}/\left(J_mN^2 + J_t\right) \quad (17)$$

$$f_3 = (NB_{mo} + B_{mo})/\left(J_mN^2 + J_t\right) \quad (18)$$

3. CONTROL DESIGN FOR ELECTRONIC THROTTLE VALVE SYSTEM

In this part, the control design is developed based on synergetic control theory. Two versions of synergetic controllers are presented: the classical synergetic control (CSC) and adaptive synergetic control (ASC). The latter is developed to cope with the uncertainties in the system parameters [14–21].

3.1. Synergetic controller (CSC)

Let ε be the error between the actual angle position $x_1 = \theta$ and the desired $x_{1d} = \theta_d$ as follows:

$$\varepsilon = x_1 - x_{1d} \tag{19}$$

The first and second time derivative of error can be given by

$$\dot{\varepsilon} = \dot{x}_1 - \dot{x}_{1d} = x_2 - \dot{x}_{1d} \tag{20}$$

$$\ddot{\varepsilon} = \dot{x}_2 - \dot{x}_{1d} = f + bu - \dot{x}_{1d} \tag{21}$$

The definition of the Marco variable $\varphi(\varepsilon)$ will be defined as

$$\varphi(\varepsilon) = \alpha\varepsilon + \dot{\varepsilon} \tag{22}$$

Taking the first time derivative of Eq. (22) to have

$$\dot{\varphi} = \dot{\varepsilon} + \alpha\ddot{\varepsilon} \tag{23}$$

where α is a scalar design for synergetic control. The definition of the $\varphi(\varepsilon)$ with respect to the manifolds is defined by

$$T\dot{\varphi} + \varphi = 0 \tag{24}$$

where T has positive real constant and it represents the converging ratio of $\varphi(\varepsilon)$ to manifold with $\varphi\ (\varepsilon) = 0$. Using Eq. (22), Eq. (23) and Eq. (24), one can get

$$T\left(\dot{\alpha\varepsilon} + \ddot{\varepsilon}\right) + \varphi = 0 \tag{25}$$

Using Eq. (9), Eq. (21) and Eq. (22), one can get

$$T\dot{\varepsilon} + T\alpha f + T\alpha bu - T\alpha\ddot{x}_{1d} + \varphi = 0 \tag{26}$$

Substituting Eq. (19) into Eq. (26) to have

$$u = \frac{1}{b_1}\left(-T\dot{\varepsilon} - T\alpha f - \varphi + T\alpha\ddot{x}_{1d}\right) \tag{27}$$

where u is the control signal that is being used. In order to achieve the desired result to satisfy

$$T\dot{\varphi} + \varphi = 0.$$

According to Eq (27), a control law can also be developed in the following way:

$$u = \frac{1}{b_1}\left(-\alpha\dot{\varepsilon} - \frac{\varphi}{T} + a_1x_1 + a_2x_2 - w - T\alpha\ddot{x}_{1d}\right) \tag{28}$$

3.2. Adaptive synergetic control design

If $\widehat{a}_1$ stands for the estimated value of the actual coefficient a_1, $\widehat{a}_2$ is the estimated value of the actual coefficient a_2, and $\widehat{w}$ stands for the estimated value of the actual coefficient w, then one can describe the estimation errors of coefficients $\tilde{a}_1$, $\tilde{a}_2$ and $\tilde{w}$, respectively, as follows [22–26]:

$$\tilde{a}_1 = \widehat{a}_1 - a_1 \tag{29}$$

$$\tilde{a}_2 = \widehat{a}_2 - a_2 \tag{30}$$

$$\tilde{w} = \widehat{w} - w \tag{31}$$

One possible definition for the candidate L.F. is

$$V = \frac{1}{2}\varphi^2 + \frac{1}{2}{\gamma_1}^{-1}{\widehat{a}_1}^2 + \frac{1}{2}{\gamma_2}^{-1}{\widehat{a}_2}^2 + \frac{1}{2}{\gamma_3}^{-1}\widehat{w}^2 \tag{32}$$

where, γ_1, γ_2, and γ_3 are the adaptation gain respectively. When we take the time derivative of Eq. (32), we get

$$\dot{V} = \varphi\dot{\varphi} - {\gamma_1}^{-1}\tilde{a}_1\dot{\widehat{a}}_1 - {\gamma_2}^{-1}\tilde{a}_2\dot{\widehat{a}}_2 - {\gamma_3}^{-1}\tilde{w}\dot{\widehat{w}} \tag{33}$$

Based on Eq. (8) and Eq. (27), one can get

$$\dot{V} = \varphi\left(\dot{\alpha\varepsilon} + \ddot{\varepsilon}\right) - {\gamma_1}^{-1}\tilde{a}_1\dot{\widehat{a}}_1 - {\gamma_2}^{-1}\tilde{a}_2\dot{\widehat{a}}_2 - {\gamma_3}^{-1}\tilde{w}\dot{\widehat{w}} \tag{34}$$

Substituting Eq. (22) in Eq. (34) to have

$$\begin{aligned}\dot{V} = \varphi&\left(\dot{\alpha\varepsilon} - a_1x_1 - a_2x_2 + \frac{1}{b_1}u + w - \ddot{x}_{1d}\right)\\ &- {\gamma_1}^{-1}\tilde{a}_1\dot{\widehat{a}}_1 - {\gamma_2}^{-1}\tilde{a}_2\dot{\widehat{a}}_2 - {\gamma_3}^{-1}\tilde{w}\dot{\widehat{w}}\end{aligned} \tag{35}$$

In case of indeterminate measure, the control law is fed estimated values of a_1, a_2 and w.

$$u = \frac{1}{b_1}\left(-\alpha\dot{\varepsilon} - \frac{\varphi}{T} + \widehat{a}_1x_1 + \widehat{a}_2x_2 - \widehat{w} - T\alpha\ddot{x}_{1d}\right) \tag{36}$$

Equation (36), which depicts the control law, allows one to derive

$$\begin{aligned}\dot{V} = \varphi&\left(\dot{\alpha\varepsilon} - a_1x_1 - a_2x_2 + \frac{1}{b_1}\left(\frac{1}{b_1}\left(-\alpha\dot{\varepsilon} - \frac{\varphi}{T} + \widehat{a}_1x_1\right.\right.\right.\\ &\left.\left.\left.+ \widehat{a}_2x_2 - \widehat{w} - T\alpha\ddot{x}_{1d}\right)\right) + w - \ddot{x}_{1d}\right)\right) - {\gamma_1}^{-1}\tilde{a}_1\dot{\widehat{a}}_1\\ &- {\gamma_2}^{-1}\tilde{a}_2\dot{\widehat{a}}_2 - {\gamma_3}^{-1}\tilde{w}\dot{\widehat{w}}\end{aligned} \tag{37}$$

$$\begin{aligned}\dot{V} = -\frac{\varphi^2}{T} &+ \varphi((-a_1x_1 - a_2x_2 + w) + (\widehat{a}_1x_1 + \widehat{a}_2x_2 - \widehat{w}))\\ &- {\gamma_1}^{-1}\tilde{a}_1\dot{\widehat{a}}_1 - {\gamma_2}^{-1}\tilde{a}_2\dot{\widehat{a}}_2 - {\gamma_3}^{-1}\tilde{w}\dot{\widehat{w}}\end{aligned} \tag{38}$$

Equation (38) can also be rewritten as

$$\begin{aligned}\dot{V} = -\frac{\varphi^2}{T} &+ \varphi(\varepsilon)((-a_1x_1 + \widehat{a}_1x_1) + (\widehat{a}_2x_2 - a_2x_2)(w - \widehat{w}))\\ &- {\gamma_1}^{-1}\tilde{a}_1\dot{\widehat{a}}_1 - {\gamma_2}^{-1}\tilde{a}_2\dot{\widehat{a}}_2 - {\gamma_3}^{-1}\tilde{w}\dot{\widehat{w}}\end{aligned} \tag{39}$$

According to Eq. (29), Eqs. (30) and (31) can be rewritten as

$$\begin{aligned}\dot{V} = -\frac{\varphi^2}{T} &+ \varphi((\tilde{a}_1)x_1 + (\tilde{a}_2x_2) - (\tilde{w})) - {\gamma_1}^{-1}\tilde{a}_1\dot{\widehat{a}}_1\\ &- {\gamma_2}^{-1}\tilde{a}_2\dot{\widehat{a}}_2 - {\gamma_3}^{-1}\tilde{w}\dot{\widehat{w}}\end{aligned} \tag{40}$$

$$\begin{aligned}\dot{V} = -\frac{\varphi^2}{T} &+ \varphi\tilde{a}_1x_1 + \varphi\tilde{a}_2x_2 - \varphi\tilde{w} - {\gamma_1}^{-1}\tilde{a}_1\dot{\widehat{a}}_1 - {\gamma_2}^{-1}\tilde{a}_2\dot{\widehat{a}}_2\\ &- {\gamma_3}^{-1}\tilde{w}\dot{\widehat{w}}\end{aligned} \tag{41}$$

Equation (41) can be set up in the following way:

$$\dot{V} = -\frac{\varphi^2}{T} + \left(\varphi x_1 - {\gamma_1}^{-1}\dot{\hat{a}}_1\right)\tilde{a}_1 + \left(\varphi x_2 - {\gamma_2}^{-1}\dot{\hat{a}}_2\right)\tilde{a}_2 - \left(\varphi - {\gamma_3}^{-1}\dot{\hat{w}}\right)\tilde{w} \quad (42)$$

In order to guarantee that $\dot{V} \le 0$, the subsequent adaptation laws can be deduced:

$$\dot{\hat{a}}_1 = -{\gamma_1}^{-1}\varphi x_1 \quad (43)$$

$$\dot{\hat{a}}_2 = -{\gamma_2}^{-1}\varphi x_2 \quad (44)$$

$$\dot{\hat{w}} = {\gamma_3}^{-1}\varphi \quad (45)$$

By using Eq. (33), $\dot{V}$ is guaranteed negative definite, which results in asymptotic stability of the controlled system.

The suggested synergetic and adaptive synergetic control strategy is shown in the form of a schematic in Fig. 3.

4. COMPUTER SIMULATION

The MATLAB/Simulink is used for modelling and simulation of the ETV system controlled by ASC and CSC. The numerical simulation has been conducted to verify the effectiveness of both controllers (ASC and CSC). The proposed control techniques have been numerically simulated and implemented within an environment of MATLAB software [27]. The Simulink model shown in Fig. 4 simulates the adaptive synergetic controlled ETV system using Simulink library. The model is made up of a total of five components: two subsystems and three MATLAB function blocks. Table 1 lists the parameter settings for the throttle valve system (TVS) [28].

The design parameters α and T are used in the design of CSC or ETV system. For both CSC and ASC, the parameter T value has been set to $T = 0.019$ and $\alpha = 40.5$. The adaption gain γ_1 for ASC based on bicep a_1 parameter has been set to $\gamma_1 = 0.109$. The adaption gain γ_2 has been set to $\gamma_2 = 0.585$ and the adaption gain γ_3 for uncertainty w has been set to $\gamma_3 = 0.099$. The T_{af} disturbance is replicated using a sinusoidal wave input having a height of 0.2 N and a 4 rad s^{-1} frequency.

4.1. Case I: excitation by sinusoidal waveform

The simulation of controlled system has been conducted by exerting desired sinusoidal trajectory, which oscillates at 0.5 rad s^{-1} and swings between 0.1745 and 0.723 rad in the angular range. Furthermore, the conditions of 0.4363 rad start the sinusoidal desired trajectory. In Fig. 5, the open-loop response shows that the system is unstable and cannot reach the desired trajectory. The throttle valve response angle for synergetic control (CSC) and adaptive synergetic control (ASC) is shown in Fig. 6. The adaptive synergetic controller shows better transient responsiveness and resilience than the synergetic controller.

The tracking error for the ASC is demonstrated, taking into account the uncertainty in the parameter and external disturbance. In this case, the ASC controller yields a root mean square error (RMSE) value of 0.1164 rad, while the CSC gives 0.1321 rad. One can conclude that the ASC exhibits better tracking performance compared to its counterpart.

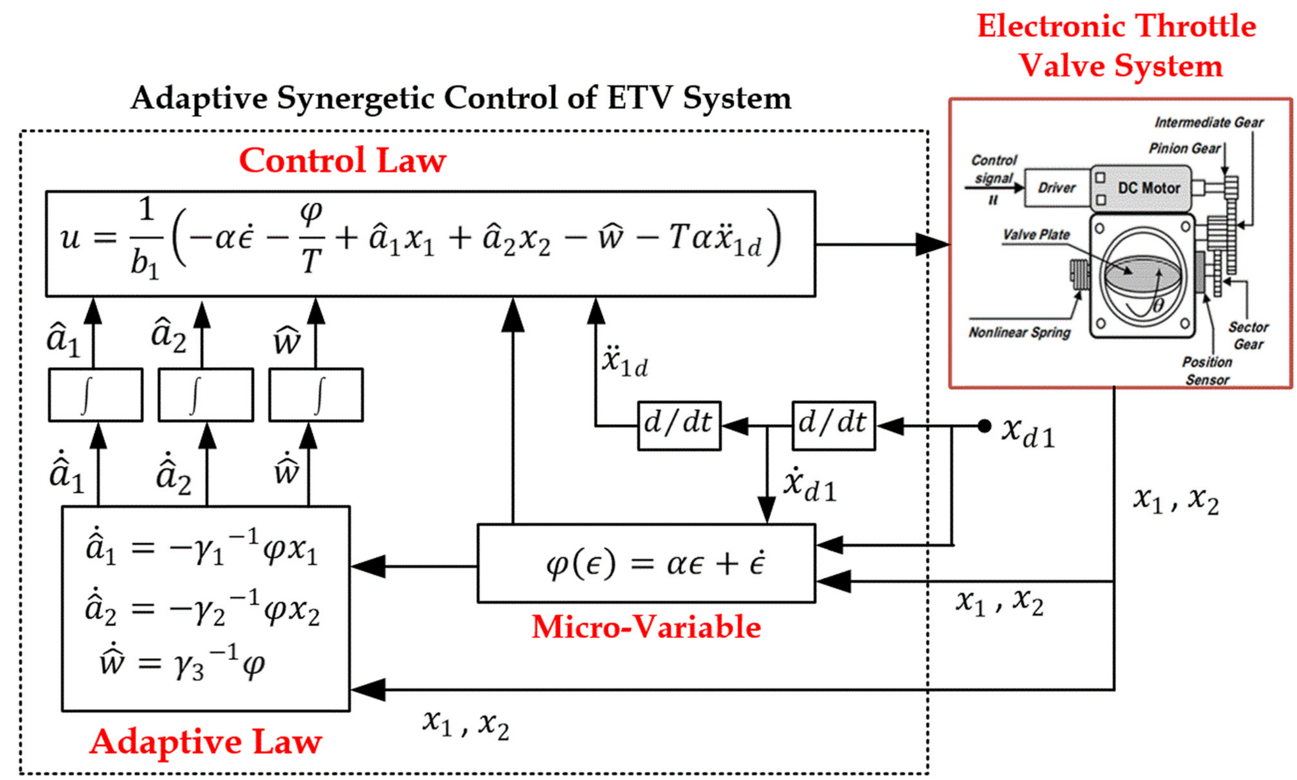

Fig. 3. The proposed adaptive synergetic control scheme for the ETV system

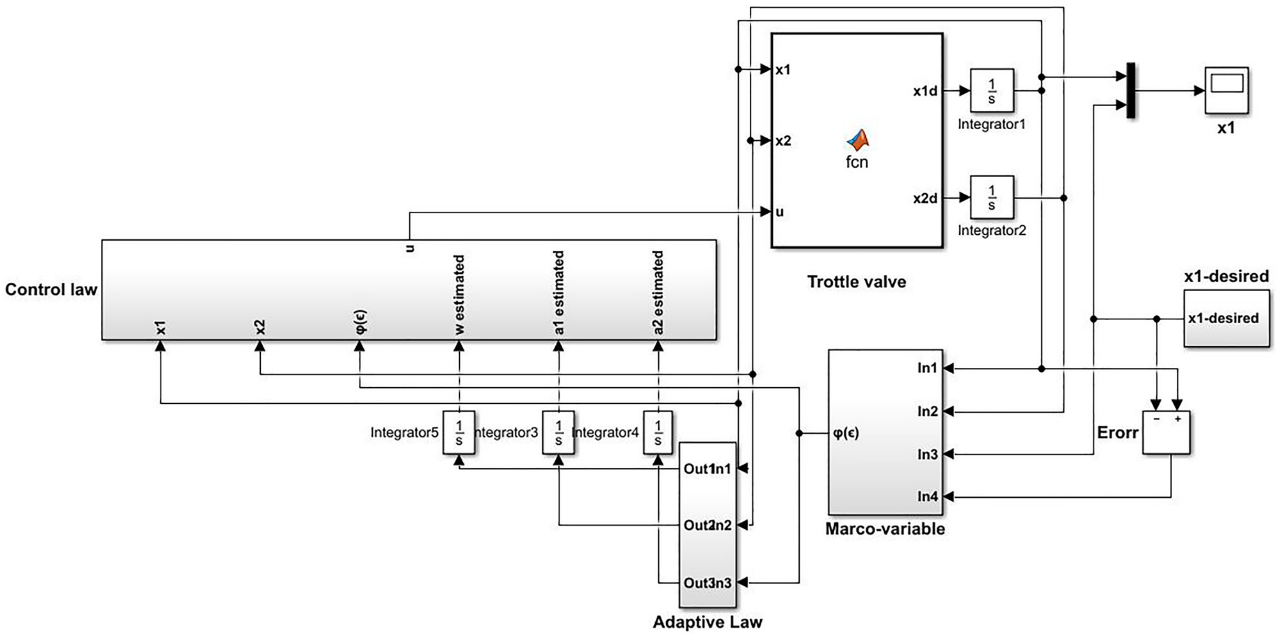

Fig. 4. Simulation modeling of ASC-based ETV system using MATLAB/Simulink

Table 1. The parameters' values of the ETV system

Parameter	Value	Parameter	Value
L	0.0017 H	J_m	0.02 Kg. m^2
R	2.1 Ω	K_t	0.072 N m A^{-1}
K_d	0.075	N	4
B_{mo}	0.006 N. m. s	K_{sp}	0.32 N m^{-1}
B_m	0.03 N. m. s	B_{to}	0.004 N. m. s
J_t	0.01 kg. m^2	B_t	0.007 N. m. s

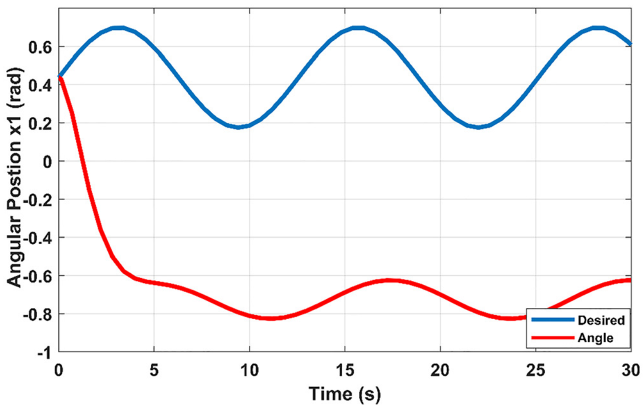

Fig. 5. Open-loop response for ETV system

Figure 7 depicts the throttle plate's angular speed response, where the adaptive synergetic controller has better transient characteristics than the synergetic controller. Figure 8 displays the behaviors of control efforts for both controllers. The figure shows that the height of spike in cases of adaptive synergetic controller is lower than that based on

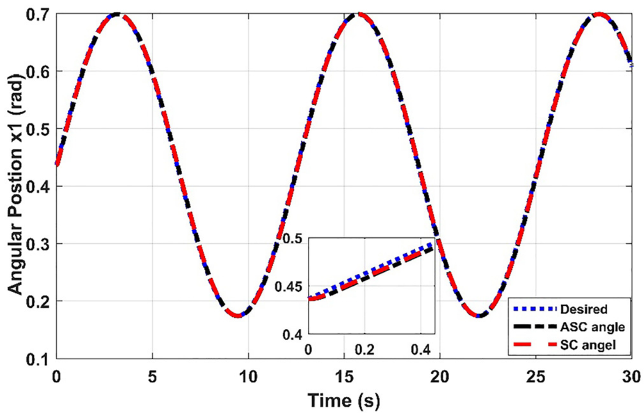

Fig. 6. Tracking performance for ETV angular position based on CSC and ASC

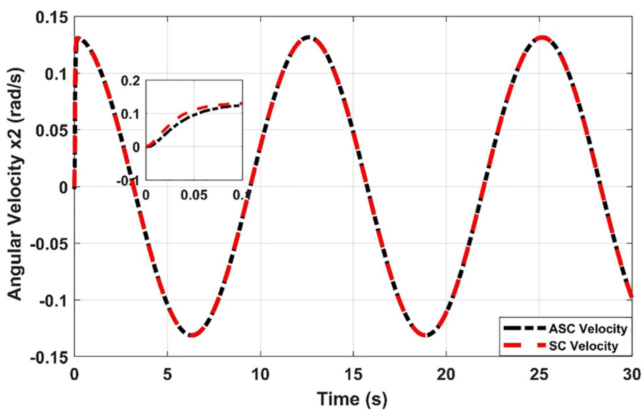

Fig. 7. Angular velocity of plate based on CSC and ASC

classical synergetic controller. In addition, the RMS of control effort for ASC is lower than that based on CSC.

Figures 9–11 illustrate, the actual and estimated values of parameters a1, a2, and w, respectively. The boundness of estimate errors for unknown parameters is one of the most important aspects to consider when assessing the performance of adaptive designs for the vast majority of adaptive controllers. If specific limits are exceeded, the regulated system's stability may be compromised. According to Figs 9–11, one can conclude that the ASC could successfully produce bounded estimated gains and it was able to prevent these gains from growing without bound. However, if the designed adaptive controller lacks the ability to confine these gains within certain bound, instability problem can occur and the controller will be infeasible in control of the electronic throttle valve.

4.2. Case II: excitation by random desired trajectory

The desired angular positions are defined by:

$$\theta_{drandom} = \frac{\pi}{6} + 0.081(\sin(2\pi F_1 t) + \sin(2\pi F_2 t) + \sin(2\pi F_3 t))$$

where, $F_1 = 0.02$, $F_2 = 0.05$ and $F_3 = 0.09$.

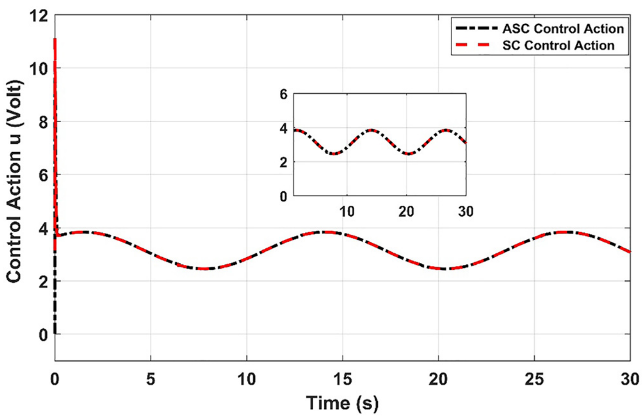

Fig. 8. Control action response based on CSC and ASC

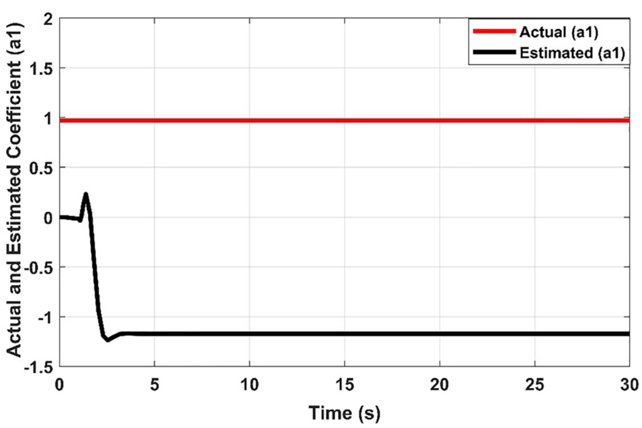

Fig. 9. Actual and estimated parameter a1

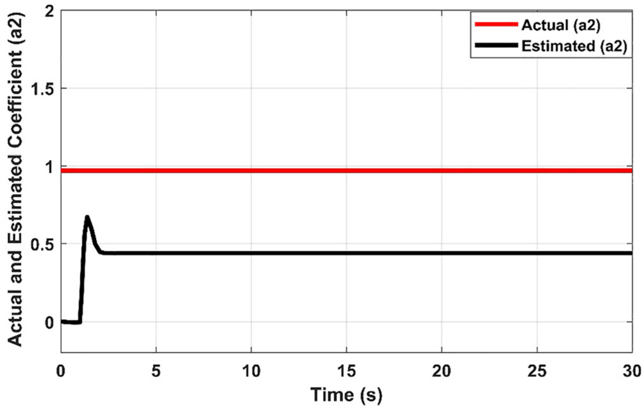

Fig. 10. Actual and estimated parameter a2

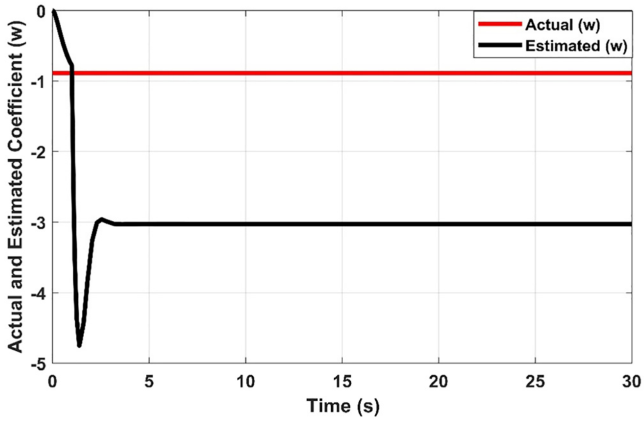

Fig. 11. Actual and estimated parameter w

Figure 12 depicts the angle position behavior based on CSC and ASC. It is evident from the zoomed-in image of the figure that the ASC performs tracking faster than that based on CSC.

The tracking error between the synergetic and adaptive controlled electronic throttle valve is shown in Fig. 13. In terms of numbers, the ASC's RMSE value is equivalent to 0.1176 rad, while the RMSE provided by CSC is equal to 0.2035 rad. This shows that the tracking performance and error variance provided by the ASC are superior to those provided by a trial-and-error method. The velocity behaviors for CSC and ASC are shown in Fig. 14. However, it is clear that CSC's peak velocity response is a little bit higher than ASC's peak velocity response. Figure 15 depicts the CSC and ASC control actions. However, the peak of the CSC control signal is slightly higher than that of the ASC signal.

5. DISCUSSION

This study made a comparison in performance between classical synergetic control (CSC) and adaptive synergetic control (ASC) in controlling the angular position of throttle valve. The ASC controller shows superior transient responsiveness and resilience compared to the CSC. The

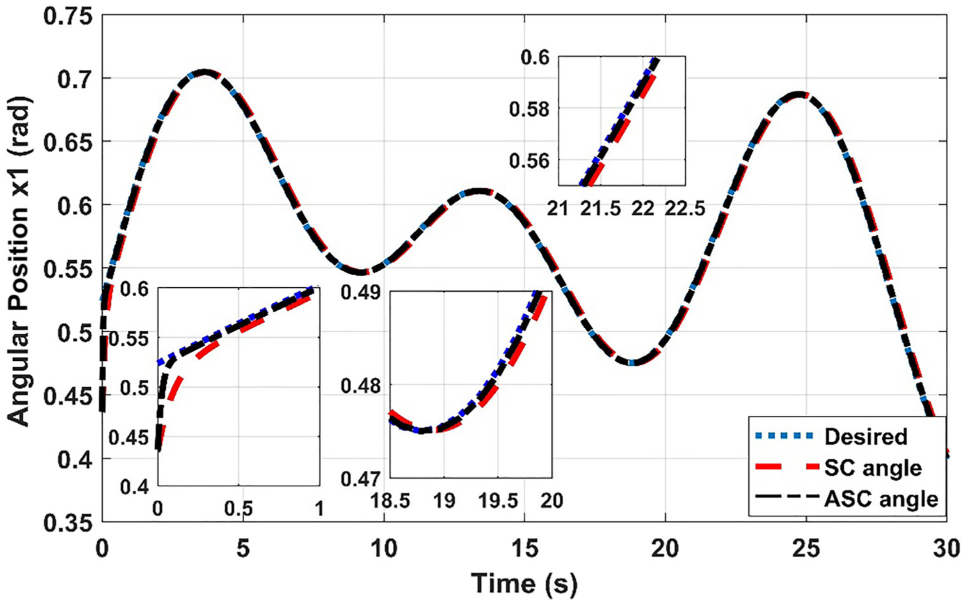

Fig. 12. Tracking performance for angular position the ETV system based on CSC and ASC with random desired

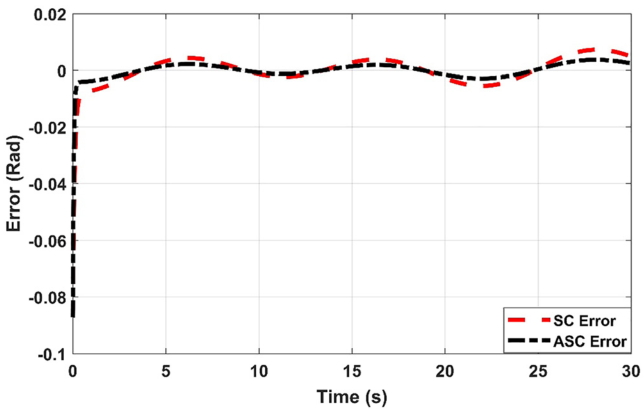

Fig. 13. Error response of plate angular position based on CSC and ASC (with random desired)

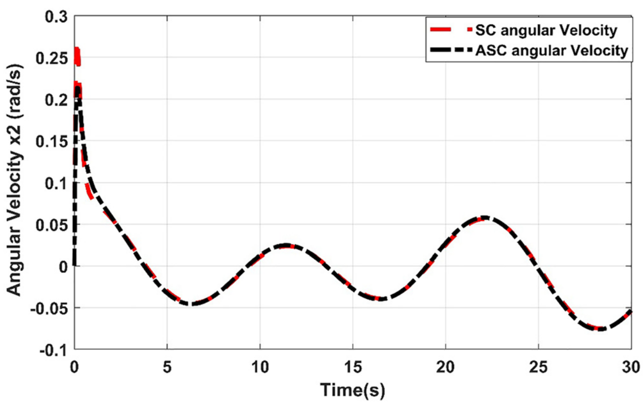

Fig. 14. Angular speed response depending on (CSC) and (ASC) with random desired

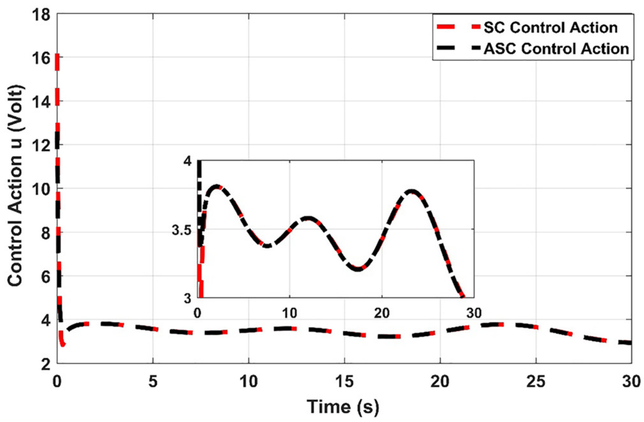

Fig. 15. Response of control action based on (CSC) and (ASC) with random desired trajectory

tracking error for ASC is 0.1164 Rad, indicating superior tracking performance and error variance. The angular speed response of the throttle plate is slightly better for ASC. The ASC requires almost the same control effort during transients, but with a lower RMSE. When tested the system with random desired wave, the tracking error of ACS is 0.1176 rad, while the CSC's RMSE is 0.2035 rad. The CSC's peak velocity response is slightly higher than the ASC's. Table 2 show RMSE value for CSC and ASC for both desired specific

Table 2. The improvements in performance

Desired Input	Controller CSC (RMSE)	Controller ASC (RMSE)	Improvement
Sinusoidal desired input	0.1321	0.1164	13.48%
Random desired input	0.2035	0.1176	11.88%

sinusoidal and random wave. The percentage difference in the RMSE values of the ASC was slightly less than that of the CSC, but when using the (ASC) it showed greater resistance to changes in the random wave and gave a value of MSMS less than CSC.

6. CONCLUSIONS

This paper presented a synergetic and adaptive synergetic control (ASC) design for electronic throttle valve system to achieve angular position tracking control. The ASC has been developed to cope with inherited uncertainty and unknown parameters. The stability analysis has been conducted to derive the control laws and adaptive laws. Two scenarios with two desired trajectories have been presented to verify the effectiveness of the proposed controllers. According to simulation results, it has been shown that the adaptive controlled system (ASC) has better tracking performance than the CSC. In case of sinusoidal waveform, the ASC shows an improvement 13.43%, while the ASC gives 11.88% improvement in the case of random desired input. Furthermore, the ASC can effectively constrain the estimation errors of uncertain parameters within defined bound to avoid the drifting problem in estimation errors, which may lead to instability of the controlled system. This study can be extended by suggesting another control scheme in the literature and a comparison study can be made with proposed controllers for the electronic throttle valve system [29–41].

REFERENCES

[1] B. Bischoff, D. Nguyen-Tuong, T. Koller, H. Markert, and A. Knoll, "Learning throttle valve control using policy search," *Lect. Notes Comput. Sci. (Including Subser. Lect. Notes Artif. Intell. Lect. Notes Bioinformatics)*, vol. 8188, LNAI, no. PART 1, pp. 49–64, 2013. https://doi.org/10.1007/978-3-642-40988-2_4.

[2] X. Yuan, Y. Wang, and L. Wu, "SVM-based approximate model control for electronic throttle valve," *IEEE Trans. Veh. Technol.*, vol. 57, no. 5, pp. 2747–56, 2008. https://doi.org/10.1109/TVT.2008.917222.

[3] M. Honek, S. Wojnar, P. Šimončič, and B. Rohaľ-Ilkiv, "Control of electronic throttle valve position of SI engine," 2010.

[4] M. Dulau and S. E. Oltean, "Simulations of robust control of the throttle valve position," May 2020. https://doi.org/10.1109/AQTR49680.2020.9129912.

[5] M. Horn, A. Hofer, and M. Reichhartinger, *Control of an Electronic Throttle Valve based on Concepts of Sliding-Mode Control*, IEEE, 2008.

[6] Q. Zeng and J. Wan, *Nonlinear PID Control of Electronic Throttle Valve Quyang*, 2011.

[7] Q. Son Tran and T. Ngoc Anh Dang, "Design of electronic throttle valve position control system using learning feed-forward based on model reference adaptive systems controller," 2016. [Online]. Available: www.ijeas.org.

[8] P. Mercorelli, "Robust feedback linearization using an adaptive PD regulator for a sensorless control of a throttle valve," *Mechatronics*, vol. 19, no. 8, pp. 1334–45, 2009. https://doi.org/10.1016/j.mechatronics.2009.08.008.

[9] W. Thanok, S. Pananurak, and M. Parnichkun, *Adaptive Cruise Control for an Intelligent Vehicle*, IEEE, 2008.

[10] R. N. K. Loh, W. Thanom, J. S. Pyko, and A. Lee, "Electronic throttle control system: modeling, identification and model-based control designs," *Engineering*, vol. 05, no. 07, pp. 587–600, 2013. https://doi.org/10.4236/eng.2013.57071.

[11] A. Shibly Ahmed Al-Samarraie, L. Yasir Khudhair Al-Nadawi, M. Hussein Mishary, and M. Mohammed Salih, "Electronic throttle valve control design based on sliding mode perturbation estimator," *Iraqi J. Comput. Commun. Control Syst. Eng. (IJCCCE)*, vol. 15, no. 2, 2015.

[12] A. J. Humaidi and A. H. Hameed, "Design and comparative study of advanced adaptive control schemes for position control of electronic throttle valve," *Information*, vol. 10, no. 2, 2019. https://doi.org/10.3390/info10020065.

[13] N. Togun and S. Baysec, "Nonlinear identification of a spark ignition engine torque based on ANFIS with NARX method," *Expert Syst.*, vol. 33, no. 6, pp. 559–68, 2016. https://doi.org/10.1111/exsy.12172.

[14] A. J. Humaidi, E. N. Talaat, M. R. Hameed, and A. H. Hameed, "Design of adaptive observer-based backstepping control of cart-pole pendulum system," in *Proceeding of IEEE International Conference on Electrical, Computer and Communication Technologies (ICECCT 2019). Coimbatore, India*. IEEE, 2019, pp. 1–5.

[15] A. J. Humaidi and M. R. Hameed, "Design and performance investigation of block-backstepping algorithms for ball and arc system," in *Proceeding of IEEE International Conference on Power, Control, Signals and Instrumentation Engineering (ICPCSI 2017). Chennai, India*. IEEE, 2017, pp. 325–32.

[16] A. J. Humaidi and A. H. Hameed, "Robustness enhancement of MRAC using modification techniques for speed control of three phase induction motor," *J. Electr. Syst.*, vol. 13, no. 4, pp. 723–41, 2017.

[17] A. J. Humaidi, and H. A. Hussein, "Adaptive control of parallel manipulator in Cartesian space," in *2019 IEEE International Conference on Electrical, Computer and Communication Technologies (ICECCT)*. Coimbatore, India, 2019, pp. 1–8.

[18] A. J. Humaidi, A. H. Hameed, and M. R. Hameed, "Robust adaptive speed control for DC motor using novel weighted E-modified MRAC," in *Proceeding of IEEE International Conference on Power, Control, Signals and Instrumentation Engineering (ICPCSI 2017), 2018*. IEEE, 2018, pp. 313–9.

[19] T. Ghanim, A. R. Ajel, and A. J. Humaidi, "Optimal Fuzzy Logic Control for Temperature Control Based on Social Spider Optimization," in *IOP Conference Series: Materials Science and Engineering*, vol. 745, 1st ed. 012099, 2020, pp. 1–15.

[20] X. Yuan, Y. Yang, H. Wang, and Y. Wang, "Genetic algorithm-based adaptive fuzzy sliding mode controller for electronic throttle valve," *Neural Comput. Appl.*, vol. 23, no. Suppl1, pp. 209–17, 2013. https://doi.org/10.1007/s00521-012-1327-1.

[21] A. J. Humaidi, S. K. Kadhim, and A. S. Gataa, "Optimal adaptive magnetic suspension control of rotary impeller for artificial heart pump," *Cybernetics Syst.*, vol. 53, no. 1, pp. 141–67, 2022. https://doi.org/10.1080/01969722.2021.2008686.

[22] A. J. Humaidi, I. K. Ibraheem, A. T. Azar, and M. E. Sadiq, "A new adaptive synergetic control design for single link robot arm actuated by pneumatic muscles," *Entropy*, vol. 22, no. 7, supp. 723, pp. 1–24, 2020. Available: https://doi.org/10.3390/e22070723.

[23] A. Q. Al-Dujaili, A. J. Humaidi, Z. T. Allawi, and M. E. Sadiq, "Earthquake hazard mitigation for uncertain building systems based on adaptive synergetic control," *Appl. Syst. Innov.*, vol. 6, no. 2, p. 34, 2023. https://doi.org/10.3390/asi6020034.

[24] S. M. Mahdi, N. Q. Yousif, A. A. Oglah, M. E. Sadiq, A. J. Humaidi, and A. T. Azar, "Adaptive synergetic motion control for wearable knee-assistive system: a rehabilitation of disabled patients," *Actuators*, vol. 11, no. 7, supp. 176, pp. 1–19, 2022. https://doi.org/10.3390/act11070176.

[25] A. S. Aljuboury, A. H. Hameed, A. R. Ajel, A. J. Humaidi, A. Alkhayyat, and A. K. A. Mhdawi, "Robust adaptive control of knee exoskeleton-assistant system based on nonlinear disturbance observer," *Actuators*, vol. 11, no. 3: (78), 2022. https://doi.org/10.3390/act11030078.

[26] R. A. Maher, E. Walid, and J. H. Amjad, "Adaptive hysteresis-band current controller," *International Journal of Power and Energy Conversion*, vol. 4, no. 4, pp. 319–38, 2013. https://doi.org/10.1504/IJPEC.2013.057033.

[27] B. Robert and E. B. Brown, *Modeling and Simulation of Systems using MATLAB and Simulink*, no. 1, 2004.

[28] R. Chen, L. Mi, and W. Tan, "Adaptive fuzzy logic based sliding mode control of electronic throttle," *J. Comput. Inf. Syst.*, vol. 8, no. 8, pp. 3253–60, 2012.

[29] N. A. Al-Awad, "Optimal controller design for reduced-order model of rotational mechanical system," *Math. Model. Eng. Probl.*, vol. 7, no. 3, pp. 395–402, September, 2020.

[30] M. Y. Hassan, A. J. Humaidi, and M. K. Hamza, "On the design of backstepping controller for Acrobot system based on adaptive observer," *Int. Rev. Electr. Eng.*, vol. 15, no. 4, pp. 328–35, 2020. https://doi.org/10.15866/iree.v15i4.17827.

[31] A. F. Hasan, et al., "Fractional Order Extended State Observer Enhances the Performance of Controlled Tri-copter UAV Based on Active Disturbance Rejection Control," in *Mobile Robot: Motion Control and Path Planning*, vol. 1090, A. T. Azar, I. Kasim Ibraheem, and A. Jaleel Humaidi, Eds., Cham: Springer, 2023. Available: https://doi.org/10.1007/978-3-031-26564-8_14.

[32] E. H. Karam, N. A. Al-Awad, and N. S. Abdul-Jaleel, "Design nonlinear model reference with fuzzy controller for nonlinear SISO second order systems," *Int. J. Electr. Comput. Eng. (IJECE)*, vol. 9, no. 4, Aug. 2019.

[33] N. Ahmed Alawad and A. Jebar, "Optimal control of model reduction binary distillation column," *I.J. Mod. Educ. Comput. Sci.*, vol. 1, pp. 59–68, 2021.

[34] Z. A. Waheed and A. J. Humaidi, "Design of optimal sliding mode control of elbow wearable exoskeleton system based on whale optimization algorithm," *J. Européen des Systèmes Automatisés.*, vol. 55, no. 4, pp. 459–66, 2022.

[35] N. Ahmad Alawad and N. Ghani Rahman, "Design of (FPID) controller for automatic voltage regulator using differential evolution algorithm," *I.J. Mod. Educ. Comput. Sci.*, vol. 12, pp. 21–8, 2019.

[36] M. N. Ajaweed, M. T. Muhssin, A. J. Humaidi, and A. H. Abdulrasool, "Submarine control system using sliding mode controller with optimization algorithm Indonesian," *J. Electr. Eng. Comput. Sci.*, vol. 29, no. 2, pp. 742–52, 2023. http://doi.org/10.11591/ijeecs.v29.i2.

[37] N. M. Noaman, A. S. Gatea, A. J. Humaidi, S. K. Kadhim, and A. F. Hasan, "Optimal tuning of PID-controlled magnetic bearing system for tracking control of pump impeller in artificial heart," *J. Européen des Systèmes Automatisés*, vol. 56, no. 1, pp. 21–7, 2023. https://doi.org/10.18280/jesa.560103.

[38] N. Q. Yousif, A. F. Hasan, A. H. Shallal, A. J. Humaidi, and L. T. Rasheed, "Performance improvement of nonlinear differentiator based on optimization algorithms," *J. Eng. Sci. Technol.*, vol. 18, no. 3, pp. 1696–712, 2023.

[39] N.A. Al-awad, A. Mohsen Abbass, M. Eddan Dubkh, "PID controller design for a magnetic levitation system using an intelligent optimization algorithm", *Int. J. Simulation: Syst. Sci. Technol. (IJSSST)*, vol. 19, no. 1, Feb.2018.

[40] A. J. Humaidi, S. K. Kadhim, M. E. Sadiq, S. J. Abbas, A. Q. Al-Dujaili, and A. R. Ajel, "Design of optimal sliding mode control of PAM-actuated hanging mass," *ICIC Express Lett.*, vol. 16, no. 11, pp. 1193–204, 2022. https://doi.org/10.24507/icicel.16.11.1193.

[41] A. J. Humaidi, S. Hasan, and A. A. Al-Jodah, "Design of second order sliding mode for glucose regulation systems with disturbance," *International Journal of Engineering and Technology (UAE)*, vol. 7, no. 2, pp. 243–7, 2018. https://doi.org/10.14419/ijet.v7i2.28.12936.